JOURNAL OF VIROLOGY, Aug. 2006, p. 7952–7964 Vol. 80, No. 16
0022-538X/06/$08.00+0 doi:10.1128/JVI.00153-06

A 38-Amino-Acid Sequence Encompassing the Arm Domain of the *Cucumber Necrosis Virus* Coat Protein Functions as a Chloroplast Transit Peptide in Infected Plants

Yu Xiang, Kishore Kakani, Ron Reade, Elizabeth Hui, and D'Ann Rochon*

Agriculture and Agri-Food Canada, Pacific Agri-Food Research Centre, Summerland, British Columbia V0H 1Z0, Canada

Received 23 January 2006/Accepted 9 May 2006

Experiments to determine the subcellular location of the coat protein (CP) of the tombusvirus *Cucumber necrosis virus* (CNV) have been conducted. By confocal microscopy, it was found that an agroinfiltrated CNV CP-green fluorescent protein (GFP) fusion targets chloroplasts in *Nicotiana benthamiana* leaves and that a 38-amino-acid (aa) region that includes the complete CP arm region plus the first 4 amino acids of the shell domain are sufficient for targeting. Western blot analyses of purified and fractionated chloroplasts showed that the 38-aa region directs import to the chloroplast stroma, suggesting that the CNV arm can function as a chloroplast transit peptide (TP) in plants. Several features of the 38-aa region are similar to features typical of chloroplast TPs, including (i) the presence of an alanine-rich uncharged region near the N terminus, followed by a short region rich in basic amino acids; (ii) a conserved chloroplast TP phosphorylation motif; (iii) the requirement that the CNV 38-aa sequence be present at the amino terminus of the imported protein; and (iv) specific proteolytic cleavage upon import into the chloroplast stroma. In addition, a region just downstream of the 38-aa sequence contains a 14-3-3 binding motif, suggesting that chloroplast targeting requires 14-3-3 binding, as has been suggested for cellular proteins that are targeted to chloroplasts. Chloroplasts of CNV-infected plants were found to contain CNV CP, but only the shell and protruding domain regions were present, indicating that CNV CP enters chloroplasts during infection and that proteolytic cleavage occurs as predicted from agroinfiltration studies. We also found that particles of a CNV CP mutant deficient in externalization of the arm region have a reduced ability to establish infection. The potential biological significance of these findings is discussed.

Viruses are highly dependent on specific host cell components for multiplication and spread. For example, replication of viral RNA by the viral RNA-dependent RNA polymerase must occur in conjunction with host proteins in a complex anchored to specified intracellular membranes (1, 8, 26, 27, 34, 41; D. Rochon, unpublished data). Similarly, movement of plant viruses from cell to cell requires precise interactions between virus-encoded movement proteins and components of the plasmadesmata and plant cell cytoskeleton (20). Entry of animal viruses into cells requires extracellular receptors for recognition and import of virus particles (14). Plant viruses do not use extracellular receptors for virus entry; rather, it is believed that disassembly of the tightly packed virus particle involves yet-to-be-identified cellular proteins and/or membrane systems. It is expected that a diversity of cellular proteins and membrane systems will be recognized as being relevant for virus multiplication in cells.

Cucumber necrosis virus (CNV), a member of the *Tombusvirus* genus of the family *Tombusviridae*, is an icosahedral virus that encapsidates a 4.7-kb single-stranded RNA genome (33). CNV is naturally transmitted by zoospores of the fungus *Olpidium bornovanus* but can also be mechanically transmitted under laboratory conditions (32). The CNV genome contains five open reading frames (ORFs) which, in addition to encoding the viral coat protein (CP), encode proteins involved in viral RNA replication, cell-to-cell movement, and suppression of gene silencing. Replication of CNV, as well as other tombusviruses, is believed to occur on peroxisomal membranes wherein viral RNA and virus-encoded components of the replicase complex have been found (26; D. Rochon, unpublished data). Specific host components have also been suggested to be involved in tombusvirus cell-to-cell movement, possibly involving interaction of the virus-encoded movement protein with a host homeodomain protein (9). The CNV p20 protein, as well as its homolog in other tombusviruses, modulates symptom induction and is a potent suppressor of gene silencing (Y. Xiang and D. Rochon, unpublished data) (19, 39, 42). In CNV, and other plant viruses as well, very little is known about the contribution of components of plant cells to the particle assembly and disassembly process.

CNV mutants that cannot produce virions can replicate and spread from cell to cell; however, virion formation is required for phloem-mediated long-distance movement (24, 36). Studies of the soil-mediated spread of CNV by zoospores of its fungal vector have suggested the involvement of specific components of the virus capsid, as well as the zoospore membrane, in virus attachment and transmission (18, 32). We have recently shown that fungus transmission requires the ability of particles to externalize a portion of the CNV CP RNA-binding (R) domain and arm domain during the zoospore membrane attachment phase (17, 32). In this study, we report that CNV CP targets chloroplasts in the leaves of infected plants and that a 38-amino-acid (aa) region encompassing the arm region is

* Corresponding author. Mailing address: Agriculture and Agri-Food Canada, Pacific Agri-Food Research Centre, Summerland, British Columbia V0H 1Z0, Canada. Phone: (250) 494-6394. Fax: (250) 494-0755. E-mail: rochonda@agr.gc.ca.

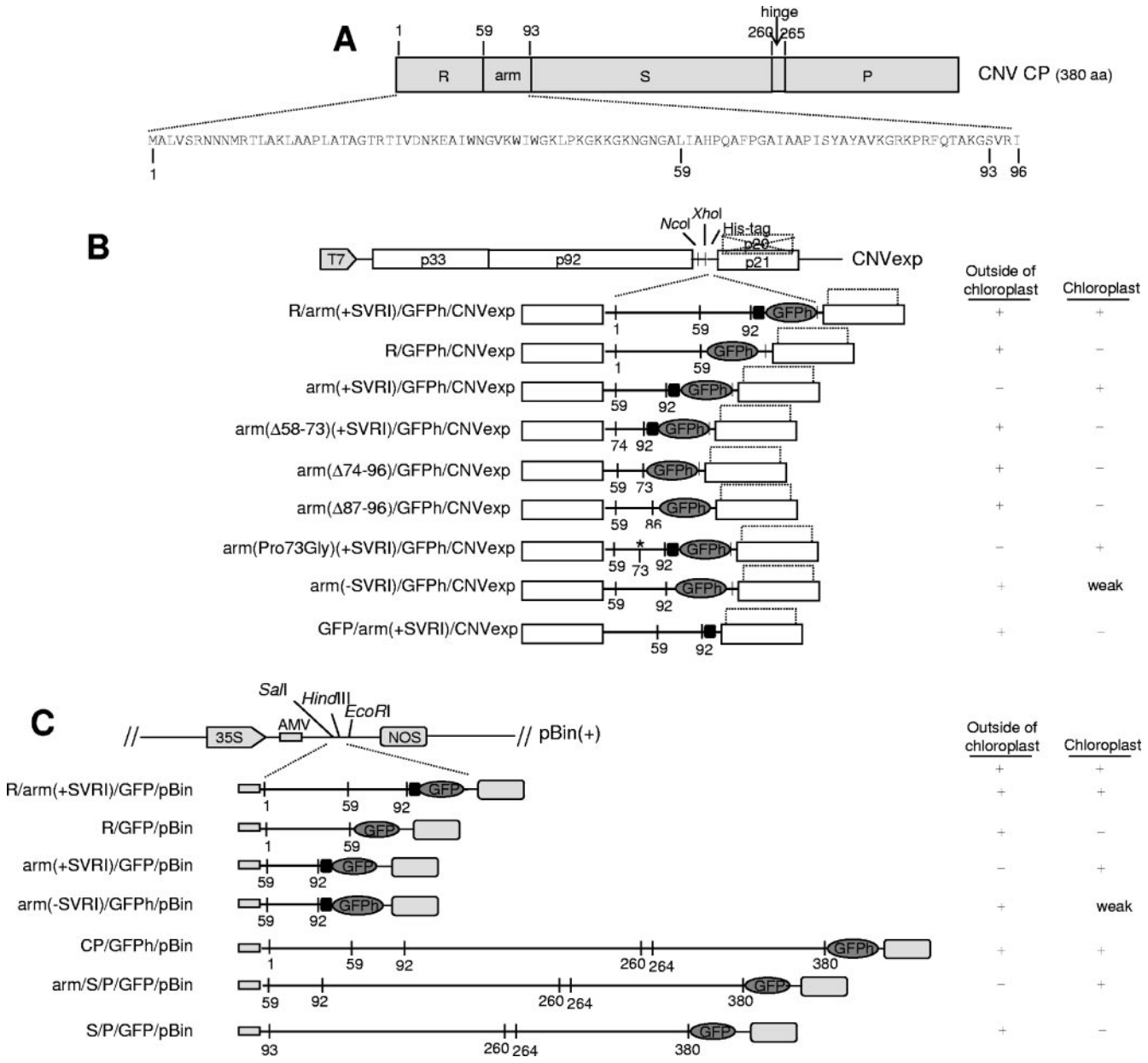

FIG. 1. Diagrammatic representation of CNV CP GFP fusion constructs. (A) Linear structure of the CNV CP subunit. The locations of the three major domains (R, S, and P), along with the connecting arm and hinge (h) regions, are shown. The amino acid sequence of the R and arm regions and the SVRI sequence of the S domain is shown below the linear structure. Numbers indicate the beginning of each of the domains. (B) Structure of CNV vector constructs used for expressing the GFP fusion proteins. p33, p92, p21, and p20 are CNV-encoded proteins. The p20 protein is not expressed in any of the constructs. The CNV CP is deleted in the CNV vector construct and is replaced by the various R- and arm-GFP fusions inserted in-frame with the CNV CP AUG initiator codon (NcoI site). The GFP in these constructs [with the exception of GFP/arm(+SVRI)/CNVexp] was His tagged at the carboxyl terminus (GFPh). The regions in the R or arm region that are retained in each construct are indicated by numbers. The small black boxes indicate the presence of the SVRI sequence of the S domain, and the ovals represent the fused GFP protein. Construct names are indicated. A summary of the locations of fusion proteins in cells is shown at the right. "Outside of chloroplast" indicates that GFP fluorescence was found in undefined locations outside of the chloroplast. (C) Structure of pBin-GFP fusion vector constructs used for expressing R- and arm-GFP fusions. See panel B for details. His-tagged GFP constructs are indicated.

both necessary and sufficient for targeting. The potential significance of this finding to the CNV infection cycle is discussed.

MATERIALS AND METHODS

Preparation of constructs for CNV-mediated expression in plants. An infectious CNV cDNA clone containing a knockout mutation in the CNV p20 ORF (33) was modified for expression of green fluorescent protein (GFP) as follows. The region containing the CNV CP initiator codon was modified to an NcoI site by oligonucleotide-directed mutagenesis, as previously described (17), and an XhoI site was similarly introduced 32 nucleotides (nt) upstream of the CP ORF stop codon. A 6-aa His tag followed by a stop codon was placed immediately after the XhoI site. (Relevant features of the construct are shown in Fig. 1.) The R-arm region (plus the first 4 aa [SVRI] of the shell [S] domain) was constructed

by insertion of its corresponding PCR fragment into CNVexp, followed by an in-frame insertion of PCR-amplified GFP. The various inserts (see Fig. 1) were prepared by PCR of the CNV CP ORF using primers containing NcoI and XhoI sites. The PCR products were then cloned into CNVexp. All constructs were sequenced to confirm the intended construction and sequence of inserts. T7 polymerase runoff transcripts were synthesized and used for inoculation of *Nicotiana benthamiana* leaves, as previously described (33).

Preparation of *Agrobacterium* binary vector constructs for agroinfiltration. pBin(+) constructs (see Fig. 1) were prepared as follows. Inserts were prepared as described above by PCR of the fusion protein ORF of CNVexp using primers that contain NcoI and BamHI sites at the 5′ and 3′ termini, respectively. The PCR products were cloned into the NcoI and BamHI sites of the intermediate vector pBBI525. The plasmid was then digested with either HindIII and EcoRI or SalI and EcoRI and inserted into the corresponding sites of the binary vector pBin(+) (38). All constructs were confirmed by sequencing for proper construction and nucleotide sequences.

The various pBin(+) constructs were transformed into *Agrobacterium* sp. strain GV3101/c58c1 (PMP90), and selected single colonies were grown at 28°C in 4 ml of YEB medium (0.1% yeast extract, 0.5% beef extract, 0.5% peptone, 0.5% sucrose, and 2 mM Mg_2SO_4) containing 50 μg/ml kanamycin and 40 μg/ml rifampin. The overnight culture was then used to inoculate 50 ml of YEB medium containing 50 μg/ml kanamycin, 40 μg/ml rifampin, 10 mM MES (morpholineethanesulfonic acid), and 20 μM acetosyringone. After overnight incubation at 28°C, *Agrobacterium* cells were harvested and resuspended in infiltration medium (10 mM $MgCl_2$, 10 mM MES, 200 μM acetosyringone), adjusted to an optical density at 600 nm of 0.5 to 1.0, and allowed to incubate at room temperature for 3 h prior to infiltration. Generally, leaves of 4- to 5-week-old *Nicotiana benthamiana* plants were infiltrated with the *Agrobacterium* culture by a 3-ml syringe (21).

Confocal microscopy. The subcellular distribution patterns of GFP and GFP-fused proteins expressed in *N. benthamiana* leaves or purified chloroplasts were observed with a Leica SP2-AOBS confocal microscope. An excitation wavelength of 488 nm was used, and fluorescence of GFP (green) and chloroplasts (red) was observed simultaneously. Leaf samples were observed under a 63× water immersion objective.

Purification of chloroplasts. Intact *N. benthamiana* chloroplasts were isolated as described by Bruce et al. (7). Briefly, 40 g of fresh leaf tissue was homogenized in a Waring blender in 180 ml ice-cold grinding buffer (50 mM HEPES-KOH [pH 7.3], 330 mM sorbitol, 0.1% bovine serum albumin, 1 mM $MgCl_2$, 1 mM $MnCl_2$, 2 mM Na_2-EDTA, 5 mM sodium ascorbate, 0.5 mM reduced glutathione) and filtered through two layers of cheesecloth and two layers of Miracloth (Calbiochem Corp., La Jolla, Calif.); released chloroplasts were pelleted at 2,000 × *g* for 5 min at 4°C. Chloroplasts were further purified on a preformed 50% Percoll gradient, washed once with import buffer (IB) (50 mM HEPES-KOH, pH 8.0–330 mM sorbitol), and resuspended in IB. The concentration of chloroplasts was determined by measuring the concentration of chlorophyll (7).

Trypsin and thermolysin treatment of chloroplasts. Intact chloroplasts were purified as described above and treated with trypsin or thermolysin as described by Bruce et al. (7). Chloroplast suspensions were adjusted to 0.5 mg of chlorophyll/ml in 400 μl of IB and either mock incubated or incubated with 20 μg of trypsin (Sigma) or 80 μg of thermolysin (Sigma) on ice for 30 min. Following incubation, trypsin activity was stopped with 40 μg of trypsin inhibitor (Sigma) and thermolysin activity was stopped with EDTA at a final concentration of 5 mM. The reaction mixtures were subsequently incubated for 10 min on ice. Intact chloroplasts were reisolated by flotation on 40% Percoll in IB, followed by one wash with IB. The repurified chloroplasts were then treated with hypotonic lysis buffer (25 mM HEPES-KOH, pH 8.0) and incubated on ice for 10 min. The soluble and membrane fractions were separated by centrifugation at 100,000 × *g* at 4°C for 10 min. Proteins in the soluble fraction were precipitated by adding 4 volumes of acetone, followed by incubation at −20°C for at least 1 h. Proteins were pelleted by centrifugation at 20,000 × *g* for 20 min at 4°C. Fractions were resuspended in equal volumes of 1× Laemmli buffer and analyzed by sodium dodecyl sulfate-polyacrylamide gel electrophoresis (SDS-PAGE) or Western blotting as described below.

SDS-PAGE and Western blot analysis. Total leaf protein samples were prepared by grinding leaf samples (0.2 g) in liquid nitrogen, followed by the addition of 4 volumes of 1× Laemmli buffer. Samples were boiled for 10 min and then centrifuged at 10,000 × *g* for 10 min at 4°C. Total chloroplast protein was prepared from Percoll-purified chloroplasts by pelleting chloroplasts (equivalent to 200 μg of chlorophyll) at 2000 × *g* for 2 min and boiling the pellet in 400 μl of 1× Laemmli buffer. Samples were electrophoresed through SDS-polyacrylamide gels. Gels were stained with Coomassie blue to confirm the quantity and assess the quality of the proteins. Proteins were blotted onto polyvinylidene difluoride membranes and probed either with a monoclonal antibody specific to GFP (BD Biosciences) or the CNV R domain (17) or with a polyclonal antibody specific to bacterially expressed CNV S and protruding (P) domain sequences (Y. Xiang, unpublished data). Antigen-antibody complexes were detected with peroxidase-labeled goat anti-mouse or anti-rabbit antibodies (Jackson Immuno-Research Laboratories) and the Enhanced Chemiluminescence Detection System (Amersham Pharmacia Biotech).

Local lesion analysis. Wild-type (WT) CNV and Pro73Gly particles were purified from infected tissue as previously described (18). The quantity of virus was determined spectrophotometrically and then confirmed by agarose gel electrophoresis of virus particles, followed by ethidium bromide staining (18). A pilot experiment was conducted to assess the concentration range in which the number of local lesions produced by WT CNV was linearly proportional to the virus concentration. This range of concentrations was then used for local lesion analysis of WT CNV and Pro73Gly particles. Two independent experiments (using plants of approximately the same age) were conducted to compare the number of lesions produced. Each virus particle concentration (1.5 ng, 0.5 ng, or 0.166 ng) in 20 μl was inoculated onto two plants, with four leaves used from each plant. The number of local lesions was counted at 4 days postinoculation (dpi). A *t* test was used to assess whether statistically significant differences existed between the number of lesions produced by each virus. Local lesion analysis of virion RNA was as described above, using the same experimental design, following a pilot experiment using WT virion RNA. Equal concentrations of virion RNA (25, 12.5, and 6.125 ng/μl) in 10 μl of 10 mM sodium phosphate buffer, pH 7.6, from each virus were used.

RESULTS

A CNV R-plus-arm domain–GFP fusion protein localizes to chloroplasts in infected plants. The CNV particle is a $T = 3$ icosahedron consisting of 180 chemically identical 41,000-molecular-weight (41K) CP subunits. The subunit consists of three major domains: the amino-terminal 58-aa R domain, the 167-aa S domain, and the 116-aa carboxyl-terminal P domain. A flexible 34-aa arm connects the R and S domains, and a 5-aa hinge (h) connects the S and P domains (Fig. 1A). The R domain and the arm are both located within the particle interior in native virions, but upon particle expansion the complete arm and a portion of the R domain become externalized (17, 31).

To determine whether CNV CP targets specific intracellular sites during infection, the coding region for the first 96 aa of the CNV CP (which corresponds to the CNV R domain and arm region, plus the first 4 amino acids [SVRI] of the S domain) (Fig. 1A) were fused in-frame with the coding region for the jellyfish GFP. The fusion protein ORF was then inserted into an infectious CNV cDNA clone (33) that lacks the CNV CP ORF. T7 polymerase runoff transcripts of the chimeric CNV construct [R/arm(+SVRI)/GFPh/CNVexp)] (Fig. 1B) were used to inoculate leaves of *Nicotiana benthamiana*; 3 to 4 dpi, leaves were examined by confocal microscopy. The results (Fig. 2A, panel a) show that GFP fluorescence localized to chloroplasts as well as to areas outside of the chloroplast. This is in contrast to constructs expressing unfused GFP (GFPh/CNVexp), where, as expected, the fluorescence is diffuse and localized to the cytoplasm (Fig. 2A, panel d). Additional constructs that contain exclusively either the CP R domain (R/GFPh/CNVexp) or the CNV arm plus the additional SVRI sequence from the S domain [arm(+SVRI)/GFPh/CNVexp] were then made to delineate the region responsible for targeting to chloroplasts. Figure 2A (panel b) shows that the construct possessing only the R domain localized to regions surrounding the chloroplast, whereas the construct containing the arm plus the SVRI sequence targeted exclusively chloroplasts

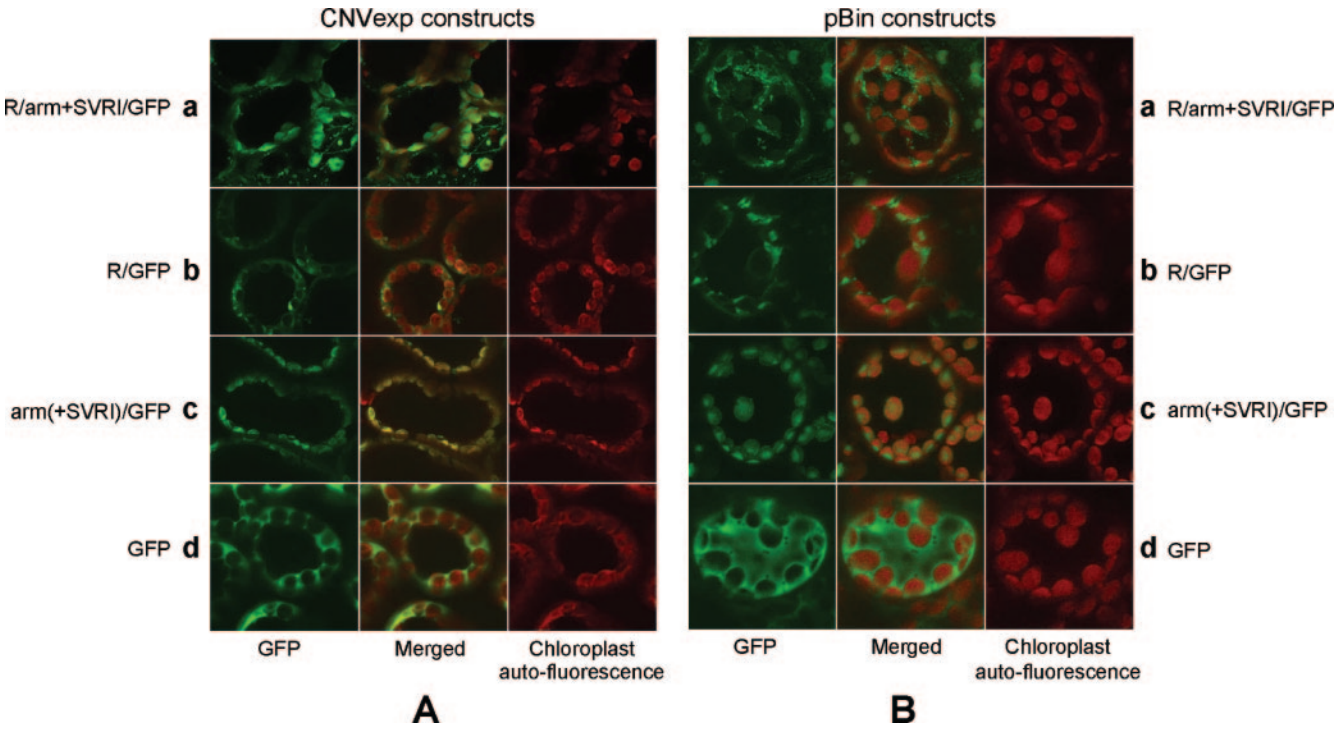

FIG. 2. Confocal images of CNV CP R and arm constructs expressed in *N. benthamiana* leaves. (A) Expression using CNVexp constructs. Leaf samples shown in panels a, b, c, and d were inoculated with RNA transcripts derived from R/arm(+SVRI)/GFPh/CNVexp, R/GFPh/CNVexp, arm(+SVRI)/GFPh/CNVexp, or GFPh/CNVexp (see Fig. 1). For each panel, the left-hand image shows GFP fluorescence (green) and the right-hand image shows chloroplast fluorescence (red). The center is a merged image of the micrographs in the left and right panels. (B) As in panel A except that leaf samples were infiltrated with R/arm(+SVRI)/GFP/pBin, R/GFP/pBin, arm(+SVRI)/GFP/pBin, or GFP/pBin (see Fig. 1).

(Fig. 2A, panel c). These results indicate that the arm domain of the CNV CP, along with the SVRI sequence from the shell (residues 58 to 96) [arm(+SVRI)], contains information that specifically targets GFP to chloroplasts.

The CNV CP arm(+SVRI) domain is sufficient for chloroplast targeting. To assess the possibility that sequences outside of the arm(+SVRI) sequence in CNVexp constructs influence targeting, regions of the GFP fusion proteins, as shown in Fig. 2A, were cloned into an *Agrobacterium tumefaciens* binary expression vector (Fig. 1C) and used to agroinfiltrate *N. benthamiana* leaves. The results, analyzed by confocal microscopy and shown in Fig. 2B, are similar to those obtained with CNV as the vector; i.e., the construct containing both the R and arm domains fused to GFP [R/arm(+SVRI)/GFP/pBin] localized to chloroplasts and structures in the vicinity of chloroplasts (Fig. 2B, panel a), the construct containing only the R domain linked to GFP [R/GFP/pBin] localized to structures outside of the chloroplast (Fig. 2B, panel b), and the construct containing only the arm(+SVRI)/GFP fusion localized primarily to chloroplasts (Fig. 2B, panel c). Together, these results indicate that the arm(+SVRI) sequence in CNV CP can target GFP to chloroplasts without the aid of other CNV-encoded proteins.

Several additional constructs were tested to further delineate amino acid sequences in arm(+SVRI) involved in chloroplast targeting (Fig. 1B): the construct arm(Δ58–73) (+SVRI)/GFPh/CNVexp lacks the amino-terminal 16 residues of the arm (+SVRI) peptide while retaining the remaining 18 aa of the arm plus the SVRI sequence of the S domain; the construct arm (Δ74–96)/GFPh/CNVexp retains only the amino-terminal 16 residues of arm(+SVRI); the construct arm (Δ87–96)/GFPh/CNVexp retains the 29 residues at the amino terminus of arm(+SVRI); and the construct arm(−SVRI)/GFPh/CNVexp contains the complete arm but lacks the SVRI region of the shell. In addition, a construct in which the arm plus the SVRI sequence are fused to the carboxyl-terminal region of GFP [GFP/arm(+SVRI)/CNVexp] was also prepared. Leaves of *N. benthamiana* were then inoculated with RNA transcripts from each construct and analyzed by confocal microscopy. Figure 1B summarizes the results and shows that of these constructs, only arm(+SVRI)/GFPh/CNVexp and arm(−SVRI)/GFPh/CNVexp targeted chloroplasts. However, targeting of arm(−SVRI)/GFPh/CNVexp was dramatically reduced in comparison to that of arm(+SVRI)/GFPh/CNVexp, with fluorescence being present primarily in the cytoplasm (see below). Notably, in GFP/arm (+SVRI)/CNVexp-inoculated plants, GFP fluorescence is found only within the cytoplasm. This observation shows that the arm(+SVRI) sequence only targets chloroplasts when present at the amino terminus of GFP.

Biochemical evidence that the CNV arm(+SVRI) sequence targets chloroplasts. Total leaf protein or protein from chloroplasts purified from *N. benthamiana* leaves infiltrated with either R/arm(+SVRI)/GFP/pBin, R/GFP/pBin, arm(+SVRI)/GFP/pBin, or GFP/pBin was extracted, electrophoresed through an SDS-polyacrylamide gel, and tested for the presence of the various GFP fusion proteins by Western blot anal-

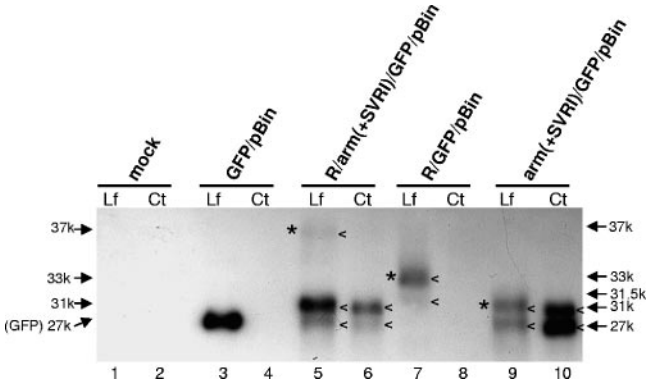

FIG. 3. Western blot analysis of total protein extracted from leaves or from purified chloroplasts of leaves agroinfiltrated with CNV CP R and arm domain-GFP fusion protein constructs. The odd-numbered lanes correspond to total leaf protein extracts (Lf), and the even-numbered lanes correspond to total protein extracted from chloroplasts (Ct). Constructs used for infiltrations are indicated above the blot for each pair of leaf or chloroplast extract shown. The Western blot was probed with a GFP monoclonal antibody. The gel was stained with Coomassie blue to ensure that each lane contained approximately the same mass of protein, as estimated by the quantity of the large subunit of ribulose bis-phosphate carboxylase (not shown). The numbers on the left correspond to the predicted masses of the proteins produced by the three GFP fusion protein constructs. The asterisks highlight the positions of the bands. The numbers on the right correspond to the approximate relative masses of the indicated proteins as determined by coelectrophoresis with molecular mass standards (not shown). The carets point to bands that are routinely observed in similar experiments.

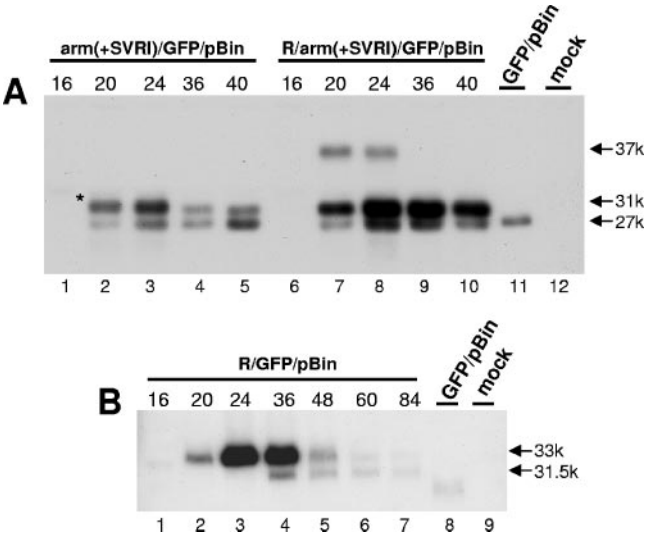

FIG. 4. Western blot analysis of total protein extracted from *N. benthamiana* leaves at several time points following infiltration. (A) Leaves were agroinfiltrated with either arm(+SVRI)/pBin (lanes 1 to 5) or R/arm(+SVRI)/pBin (lanes 6 to 10). Total leaf proteins were electrophoresed through an SDS-polyacrylamide gel, followed by Western blot analysis using a GFP monoclonal antibody. Time points are indicated in hours postinfiltration above the respective lanes. Lane 11 corresponds to a leaf sample from an *N. benthamiana* plant infiltrated with GFP/pBin, and lane 12 corresponds to uninfiltrated plants. The relative masses of CNV CP species, as estimated by coelectrophoresis of protein molecular size standards, are indicated on the right. The asterisk shows the position of a minor protein species observed in arm(+SVRI)/GFP/pBin infiltrations. (B) As in panel A except that plants were infiltrated with R/GFP/pBin.

ysis using a GFP monoclonal antibody. Figure 3 shows that GFP antibody reacted to protein species in total leaf extracts of plants infiltrated with all three GFP fusion protein constructs (lanes 5, 7, and 9) but reacted only to protein extracted from purified chloroplasts isolated from R/arm(+SVRI)/GFP/pBin and arm(+SVRI)/GFP/pBin (Fig. 3, lanes 6 and 10, respectively) (see below for further analyses of the multiple protein species detected in each lane). These results provide additional evidence that proteins produced by R/arm(+SVRI)/GFP/pBin and arm(+SVRI)/GFP/pBin both target chloroplasts and that arm(+SVRI) sequences are sufficient for this targeting. In addition, the results reinforce the conclusion that the R domain-GFP fusion targets regions outside of the chloroplast.

Fusion proteins produced by R/arm(+SVRI)/GFP/pBin, arm(+SVRI)/GFP/pBin, and R/GFP/pBin undergo specific cleavage in agroinfiltrated plants. We note that GFP fusion proteins detected in plants infiltrated with R/arm(+SVRI)/GFP/pBin unexpectedly exist as several proteins smaller than the predicted size of 37K (Fig. 3, lanes 5 and 6). Total leaf extracts contain proteins with estimated sizes of approximately 37K, 31K, and 27K (Fig. 3, lane 5), whereas chloroplast extracts contain proteins of 31K and 27K (Fig. 3, lane 6). Total leaf protein of plants agroinfiltrated with R/GFP/pBin contains primarily the predicted 33K protein (Fig. 3, lane 7) but also contain detectable levels of an approximately 31.5K protein (Fig. 3, lane 7). Neither of these proteins is detected in chloroplast extracts (Fig. 3, lane 8). Plants infiltrated with arm(+SVRI)/GFP/pBin contain a 27K protein in addition to the predicted 31K protein in both total and chloroplast protein extracts (Fig. 3, lanes 9 and 10). These results suggest that both the R and arm domains undergo specific proteolytic cleavage in agroinfiltrated plants.

A time course experiment was conducted to further investigate the precursor/product relationship between the multiple protein species present in agroinfiltrated plants. Total protein was extracted from leaves at various times postinfiltration and then analyzed by SDS-PAGE, followed by Western blotting using a GFP monoclonal antibody. As can be seen in Fig. 4A, two prominent protein species of 31K and 27K are detected in leaf extracts of arm(+SVRI)/GFP/pBin-infiltrated leaves from 20 h through 40 h postinfiltration (Fig. 4A, lanes 2 to 5). However, the relative abundance of the predicted 31K fusion protein compared to that of the 27K protein decreases over time (Fig. 4A; compare lanes 3, 4, and 5), suggesting that the 27K protein represents a cleavage product of the 31K protein. Based on the estimated size of the 27K cleavage product, cleavage is predicted to occur at or near the junction of the arm-GFP fusion (Fig. 1C). In a similar time course experiment using agroinfiltrated R/arm(+SVRI)/GFP/pBin, a protein with an estimated mass similar to that of the predicted full-length fusion protein (i.e., 37K) is present at 20 and 24 h postinfiltration (Fig. 4A, lanes 7 and 8) but is not detectable at later time points (Fig. 4A, lanes 9 and 10). Proteins with estimated sizes of 31K and 27K are observed from 20 to 40 h postinfiltration; the amount of these proteins first increases up to 24 h and then declines thereafter (Fig. 4A, lanes 6 to 10). Moreover, the ratio of the 37K protein to either the 31K or 27K protein decreases over time, consistent with a precursor/product relationship be-

tween the 37K protein and one or both of the 31K and 27K proteins. A change in the ratio of intensities between the 31K and 27K proteins is not apparent, as was observed in the arm(+SVRI)/GFP/pBin construct. However, ongoing synthesis of the 37K protein followed by its cleavage to the 31K protein complicates an analysis of the 31K/27K ratio. Based on the relative intensities of the 37K and 31K proteins, we suggest that the 31K protein is a specific cleavage product of the 37K fusion protein near the junction of the R and arm domains. Similarly, based on results observed in plants infiltrated with arm(+SVRI)/GFP/pBin, the 27K protein is likely a specific cleavage product of the 31K protein wherein cleavage is predicted to occur near the arm and GFP fusion protein junction (Fig. 1C). In addition, the presence of a 31K and 27K protein, along with the absence of the 37K species in chloroplasts, indicates that the 27K peptide is likely cleaved from the 31K protein within chloroplasts (Fig. 3). Similarly, the absence of the 37K protein in chloroplasts indicates that cleavage to the 31K protein occurs outside of the chloroplast.

Time course experiments with plants infiltrated with R/GFP/pBin show that synthesis of the predicted full-length 33K protein precedes accumulation of a 31.5K protein (Fig. 4B) and that the ratio of the 33K protein to the 31.5K protein decreases over time (Fig. 4B). This pattern of expression is consistent with the 31.5K species arising from cleavage of the 33K species within the R domain at approximately 12 to 18 amino acids from the N terminus. We also note that although the 31K cleavage product of the R/arm(+SVRI) construct was detected at about the same time as its precursor (Fig. 4A, lane 7) the cleavage product of the R-GFP construct was not visible until about 16 h after the appearance of its precursor (Fig. 4B; see lanes 2 and 4). Thus, cleavage within the R domain sequence of R-arm is not as efficient as that at the R-arm junction, and/or cleavage is delayed.

The 31.5K species is the only cleavage product detectable in R/GFP/pBin-infiltrated leaves. The absence of a cleavage product near the R-GFP junction suggests that the 31K cleavage product of R/arm(+SVRI)/GFP/pBin that was predicted to occur near the R-arm boundary likely occurs on the arm side.

The CNV arm functions as a chloroplast transit peptide (TP) that targets GFP to the stroma. To further refine the location of the arm domain and its cleavage product in chloroplasts, intact chloroplasts were purified from leaves infiltrated with R/arm(+SVRI)/GFP/pBin and were subsequently either mock incubated or incubated with thermolysin or trypsin (Fig. 5A). Thermolysin digests only those proteins associated with the chloroplast outer membrane, whereas trypsin digests proteins present on the outer membrane as well as within the chloroplast intermembrane space. Proteins present in the stromal fraction or the thylakoids are not digested by either trypsin or thermolysin (16, 22). Following protease treatment, chloroplasts were disrupted and the membrane and soluble fractions were separated. Proteins from these fractions were then analyzed by SDS-PAGE and Western blotting using a GFP monoclonal antibody. As previously observed in Fig. 3, the 37K R/arm(+SVRI)/GFP/pBin fusion protein as well as its 31K and 27K cleavage products are present in total protein extracts, but only the 31K and 27K cleavage products are associated with chloroplasts (Fig. 5A, lanes 3 and 4). Examination of the

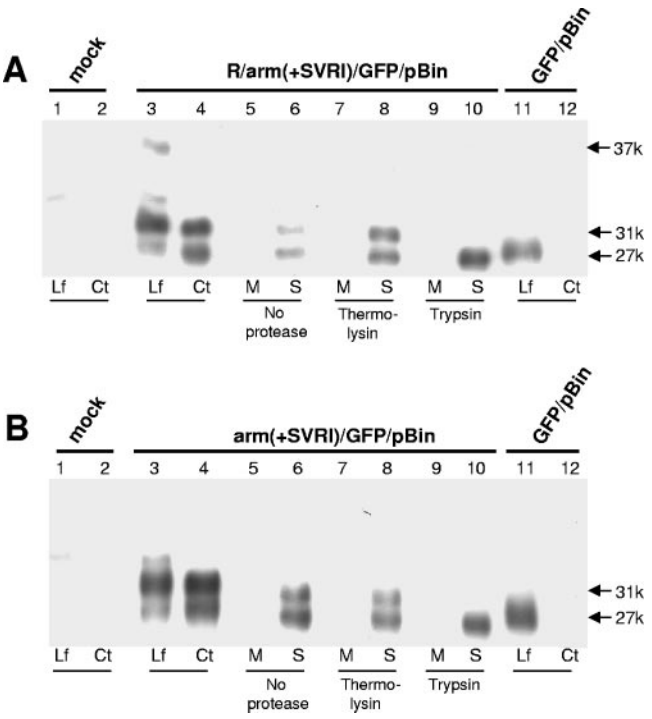

FIG. 5. Western blot analysis of the locations of R/arm(+SVRI)/GFP/pBin and arm(+SVRI)/GFP/pBin in chloroplasts of agroinfiltrated plants. Chloroplasts were isolated from infiltrated leaves (24 h postinfiltration) and treated with either thermolysin or trypsin, followed by centrifugation to separate the membrane (pellet) and soluble (supernatant) fractions. Lanes 3 to 10 in panel A correspond to plants infiltrated with R/arm(+SVRI)/GFP/pBin, and lanes 3–10 in panel B correspond to plants infiltrated with arm(+SVRI)/GFP/pBin. Lanes 3 and 4 of each blot correspond to total leaf protein (Lf) and total chloroplast protein (Ct), respectively. Purified chloroplasts were either mock treated (no protease) or treated with thermolysin or trypsin, followed by purification of the membrane (M) and soluble (S) fractions as indicated. Lanes 1 and 2 and lanes 11 and 12 correspond to total leaf protein and total chloroplast protein extracted from uninfiltrated or GFP/pBin-infiltrated *N. benthamiana*, respectively. The blot was probed with a GFP monoclonal antibody. The relative masses of the main protein species, as estimated by coelectrophoresis of protein molecular size standards, are indicated.

chloroplast membrane and soluble fractions shows that the 31K and 27K proteins are detected almost exclusively in the soluble fraction (Fig. 5A; compare lanes 5 and 6). Both of these proteins are resistant to thermolysin treatment (Fig. 5, lane 8), indicating that they are not associated with the chloroplast outer membrane. Figure 5A, lane 10, shows that the 31K protein is sensitive to trypsin digestion but that the 27K protein is not. This observation indicates that the 31K protein is present only in the chloroplast intermembrane space and that the 27K protein is present only in the stroma.

A similar experiment was conducted with leaf extracts from arm(+SVRI)/GFP/pBin-infiltrated plants (Fig. 5B); as with the results obtained with R/arm(+SVRI)/GFP/pBin, it was found that the 31K protein is associated only with the chloroplast intermembrane space and that the 27K protein is only within the stroma. This pattern of import is similar to that documented for several cytoplasmically synthesized chloroplast preproteins in which an N-terminal TP targets the protein

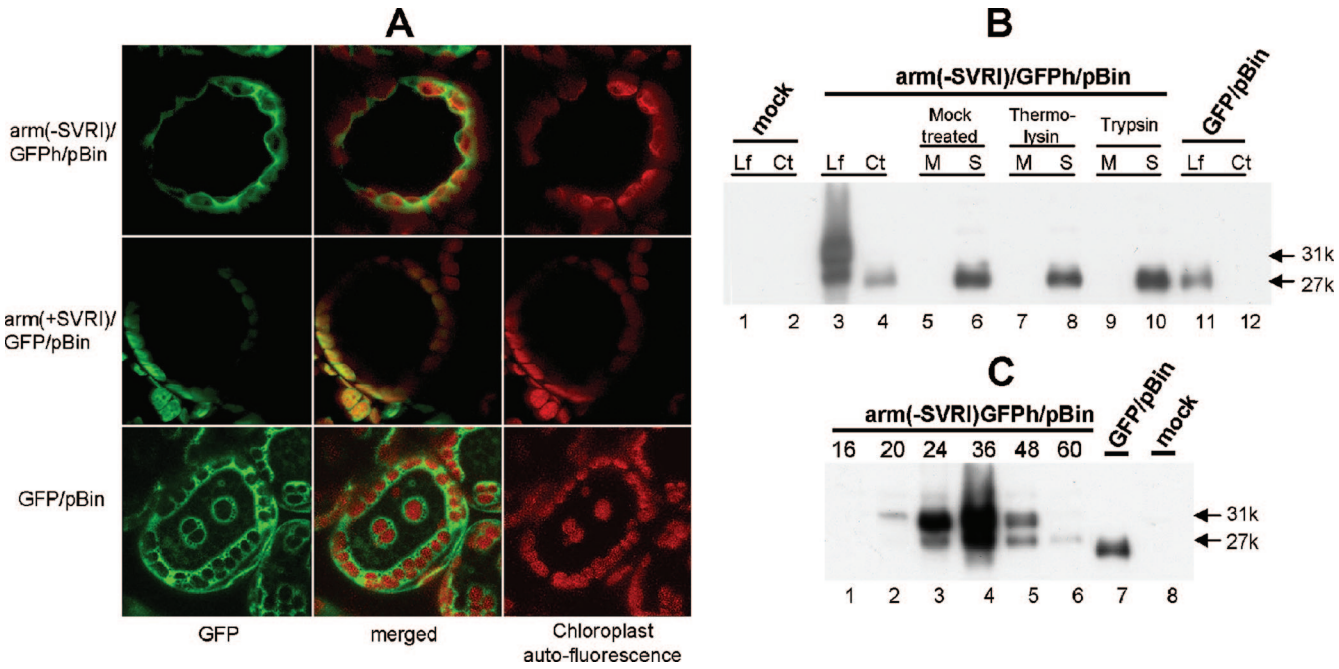

FIG. 6. Western blot analysis of the location of arm(−SVRI)/GFPh/pBin in agroinfiltrated plants and the time course of expression. (A) Confocal images of agroinfiltrated leaves of arm(−SVRI)/GFPh/pBin in comparison to arm(+SVRI)/GFP/pBin and GFP/pBin. Constructs used for agroinfiltration are shown on the left. For each panel, the left-hand image shows GFP fluorescence (green), the right-hand image shows chloroplast fluorescence (red), and the center shows a merged image. (B) Chloroplasts purified from *N. benthamiana* leaves were infiltrated with arm(−SVRI)/GFPh/pBin, and chloroplast fractions were subjected to thermolysin and trypsin treatment, as described in the legend to Fig. 5. (C) Time course analysis of plants infiltrated with arm(−SVRI)/GFPh/pBin. Experiments were conducted as described in the legend to Fig. 4.

to the chloroplast stroma, where proteolytic removal of the TP occurs (2, 22, 30, 37). Based on this and the other observations made thus far, we suggest that the CNV arm(+SVRI) sequence can function as a chloroplast TP that targets proteins to the stroma.

The SVRI sequence present in the carboxyl-terminal region of the CNV CP arm domain is essential for efficient chloroplast targeting. An experiment similar to that shown in Fig. 5 was conducted with the arm(−SVRI)/GFP/pBin construct, which lacks the SVRI sequence of the S domain (Fig. 1C). Confocal microscopy indicated that some targeting to chloroplasts occurred but that it was inefficient in comparison to the arm(+SVRI)/GFP/pBin construct, as fluorescence was found primarily in the cytoplasm (Fig. 6A). Western blot analysis showed that the 31K precursor protein and the 27K cleavage product are detected in total leaf extracts (Fig. 6B, lane 3). However, much less fusion protein is imported into chloroplasts using arm(−SVRI) construct (Fig. 6B, lanes 3 and 4) than using arm(+SVRI) construct (Fig. 5B, lanes 3 and 4). Interestingly, protein extracted from purified chloroplasts of arm(−SVRI)/GFPh/pBin-infiltrated plants contained the 27K protein (Fig. 6B, lane 4) but lacked detectable amounts of the 31K precursor, indicating that most of the arm(−SVRI)/GFPh precursor accumulates in the cytoplasm. This is in marked contrast to experiments using arm(+SVRI)/GFP/pBin constructs, in which both the 31K and 27K proteins are abundant in chloroplasts (Fig. 3, lane 10; Fig. 5B, lane 4), with the 31K protein being in the intermembrane space and the 27K protein in the stroma (Fig. 5B, lanes 8 and 10, respectively). Experiments using fractionated and protease-treated chloroplasts (Fig. 6B, lanes 5 to 10) show that the 27K protein produced by arm(−SVRI)/GFPh/pBin is present in the stromal fraction (Fig. 6B, lane 6). A densitometric analysis of Western blots, in which both sets of samples were run concurrently, was conducted, and the relative amount of protein in total leaf extracts and chloroplasts was assessed (not shown). In the case of the arm(+SVRI) construct, it was found that more than 56% of the total protein was present in the chloroplast fraction, whereas only 7% of that of the arm(−SVRI) fusion protein was found in chloroplasts (data not shown). The precursor/product relationship of the 31K and 27K proteins in arm(−SVRI)/GFP/pBin-infiltrated plants was further analyzed by examination of the relative abundance of the two proteins at different time points following infiltration. Figure 6C shows that from 20 to 48 h postinfiltration, the level of the 31K protein exceeds that of the 27K protein. By 60 h postinfiltration, only very low levels of protein are observed, with only the 27K protein being detectable.

Taken together, the confocal and Western blot analyses show that only a small percentage of the arm(−SVRI) construct enters chloroplasts and that only a 27K stromal cleavage product is detectable. These observations suggest that the 31K protein of arm(−SVRI)/GFP/pBin is inefficiently targeted to chloroplasts, but once targeted it is readily imported into the stroma. We therefore conclude that the SVRI sequence present at the carboxyl-terminal region of the arm is an important component of the CNV chloroplast targeting sequence.

GFP fusion protein constructs containing the complete CNV CP can be imported into the chloroplast stroma. The CNV CP ORF was fused to GFP (CP/GFPh/pBin) (Fig. 1C) and used to

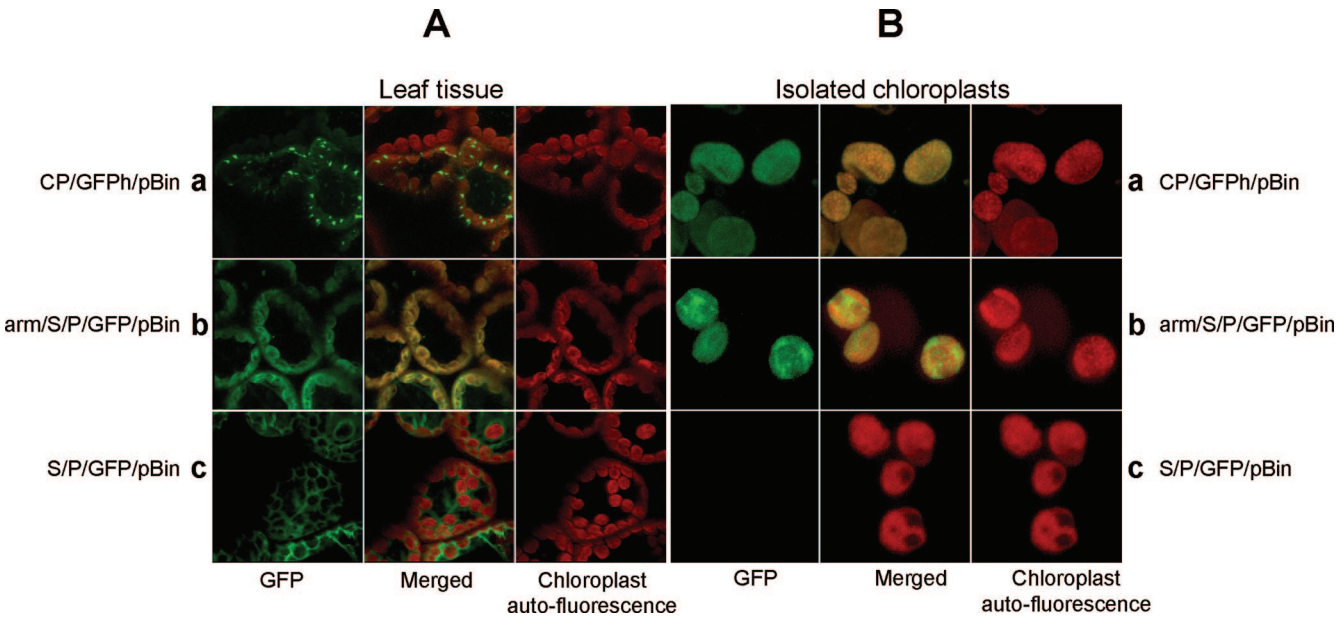

FIG. 7. Confocal images of CNV CP/GFPh/pBin, arm/S/P/GFP/pBin, and S/P/GFP/pBin constructs expressed in *N. benthamiana* leaves. Leaf samples were agroinfiltrated with the indicated constructs, and leaves were directly analyzed by confocal microscopy (A) or chloroplasts were first purified and then analyzed (B). For each panel, the left-hand image shows GFP fluorescence (green), the right-hand image shows chloroplast fluorescence (red), and the center shows a merged image.

agroinfiltrate *N. benthamiana* leaves. Confocal microscopy of infiltrated leaves (Fig. 7A, panel a) shows that GFP fluorescence is associated with discrete structures in the vicinity of chloroplasts, as well as within chloroplasts (Fig. 7A, panel a), similar to that observed previously with other CP R-arm domain constructs (Fig. 2A and B, panel a). A construct that lacks the CP R domain coding region but contains the additional downstream CP sequences along with the fused GFP ORF (i.e., arm/S/P/GFP/pBin) (Fig. 1C) shows primarily chloroplast targeting (Fig. 7A, panel b), again being similar to previous results with arm-GFP constructs (Fig. 2A and B, panel c). Another construct lacking the R domain and arm region but containing the remaining CP sequences (S/P/GFP/pBin) (Fig. 7A, panel c) was found only in the cytoplasm. We also examined chloroplasts purified from leaves agroinfiltrated with each of the constructs described above. Figure 7B shows that fluorescence is clearly found within chloroplasts of both CP/GFPh/pBin and arm/S/P/GFP/pBin (panels a and b, respectively) but is not found within chloroplasts isolated from S/P/GFP/pBin. The results therefore indicate that full-length CNV CP can also undergo import into chloroplasts.

Western blot analyses of total leaf extracts, total chloroplast extracts, and trypsin- and thermolysin-treated soluble and membrane fractions of chloroplasts of each of the constructs described above were also conducted (data not shown). The results were consistent with the results of the confocal microscopy experiments in that the CP/GFPh/pBin and arm/S/P/GFP/pBin fusion proteins both localized to the soluble fraction of chloroplasts and that S/P/pBin was restricted to the cytoplasm. In addition, proteolytic cleavages of the proteins were clearly observed (data not shown). However, due to the large sizes of the proteins being detected as well as the similarities in the sizes of cleavage products, it was not possible to ascertain the sizes of the various protein species.

CP sequences are imported into chloroplasts during CNV infection. Chloroplasts of CNV-infected *N. benthamiana* leaves were examined for the presence of CNV CP by Western blot analysis and a polyclonal antibody raised to the CNV S/P domain. Figure 8, lane 2, shows that three CNV-specific proteins (see asterisks) with estimated sizes of 41K (full-length CNV CP), 35K, and 31K are found in protein extracted from purified chloroplasts, suggesting that CNV CP sequences are indeed associated with chloroplasts in CNV-infected plants. Moreover, as observed in previous agroinfiltration experiments, imported CNV CP species are found primarily in the

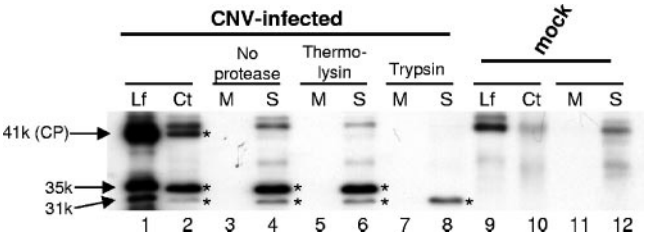

FIG. 8. Subcellular location of CNV CP in plants inoculated with CNV. Leaves were inoculated with CNV and at 2 dpi were analyzed for the location of CNV CP in total leaf extracts and in chloroplasts. The specific location of CP was assessed by trypsin and thermolysin treatment of purified chloroplasts, as described in the legend to Fig. 5. Western blots were probed with a CNV polyclonal antibody to the CNV CP S/P domain. Asterisks indicate bands that are specific to infected leaf extracts. The predicted molecular masses of the proteins are indicated on the left. The relative masses of CNV CP species, as estimated by coelectrophoresis of protein molecular mass standards, are indicated.

chloroplast soluble fraction (Fig. 8, lane 4). Figure 8, lane 6, shows that both the 35K and 31K species are resistant to thermolysin, whereas only the 31K species is resistant to trypsin treatment (Fig. 8, lane 8), suggesting that the 35K protein is present in the chloroplast intermembrane space and the 31K protein in the stroma. We were unable to detect the 35K and 31K proteins with a monoclonal antibody specific to the CNV R domain (data not shown). This, along with the fact that the sizes of these proteins closely match the predicted masses of 34.7K for the CNV arm/S/P region and 31.1K for the S/P regions, indicates that these proteins most likely correspond to cleavages near the R-arm and arm-S boundaries, respectively. It is suggested that the 35K and 31K species represent proteolytic intermediates in the import of CNV CP into chloroplasts during infection and that their cleavage sites correspond to those predicted with the R/arm(+SVRI) and arm(+SVRI) GFP fusion protein constructs. However, precise identification of the cleavage sites of the various protein species is still required.

A CNV CP arm mutant is inefficient in establishing infection in a local lesion host. To assess the possibility that targeting of CNV virions to chloroplasts may play a role in the uncoating stage of virus infection, we analyzed a previously described CNV CP arm mutant (Pro73Gly) (17) for the ability to establish infection in plants. Pro73Gly contains a glycine residue in place of a proline residue at aa 73 in the CP arm region. Previous studies showed that although mutant virus particles accumulate efficiently in *N. benthamiana*, particles fail to extrude the arm region to the outside of the particle, resulting in the inability of the particles to be transmitted to root cells following attachment to the fungal zoospore membrane (32).

Local lesion analyses were conducted to assess the ability of Pro73Gly to initiate infection in a local lesion host. We reasoned that if targeting of the arm(+SVRI) sequence to chloroplasts is an important aspect of the uncoating process, then particles of Pro73Gly would be expected to show a decrease in the number of lesions while virion RNA extracted from particles would show an equivalent number of lesions. The validity of this experimental approach is supported by the fact that CNV can efficiently replicate and move from cell to cell in the absence of the CP (25, 36). Figure 9 summarizes the results of experiments in which equal concentrations of Pro73Gly virions or extracted virion RNA was inoculated onto leaves of the local lesion host, *Chenopodium quinoa*, and the number of local lesions was compared to that of the WT. Significantly fewer local lesions were produced by virions of Pro73Gly than by WT CNV. However, when virion RNA was used as the inoculum, no significant differences in the numbers of local lesions were found. The smaller number of local lesions produced by Pro73Gly virions can be explained by the inability to establish rather than to continue infection and is therefore consistent with the involvement of the arm region in the uncoating process.

GFP fusions to the arm region of Pro73Gly, [arm(Pro73Gly)(+SVRI)/GFPh/CNVexp] were found to target chloroplasts in agroinfiltration experiments, indicating that the Pro73Gly mutation does not affect the TP function of the arm per se. Thus, the relatively low number of local lesions produced upon Pro73Gly virion inoculation is consistent with the inability of the arm to extrude to the particle surface and thereby act as a TP rather than being a result of the Pro-to-Gly substitution in the CP subunit.

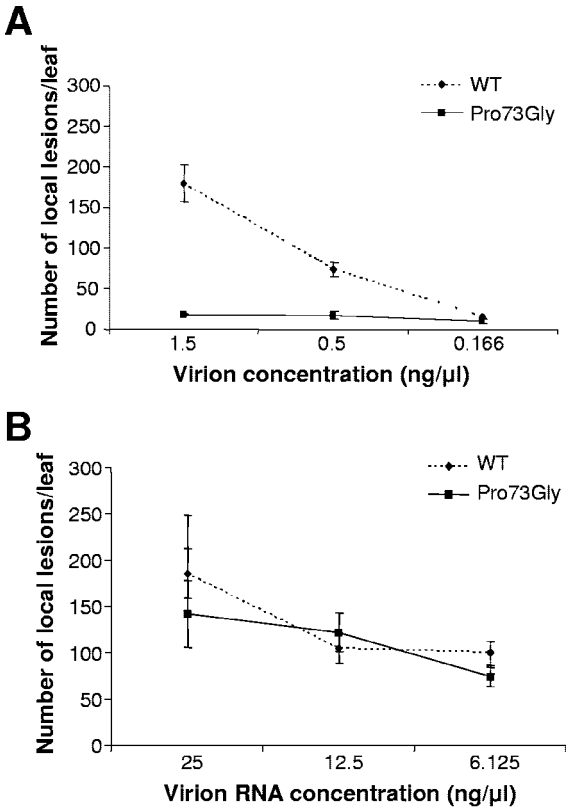

FIG. 9. Local lesion analysis of two CNV CP arm mutants. (A) Equal concentrations of WT CNV or Pro73Gly particles were inoculated onto leaves of *C. quinoa*, and the number of local lesions was determined at 4 dpi. Two independent experiments were conducted, using two plants for each treatment and four leaves per plant. (B) As in panel A except that equal concentrations of purified virion RNA were used. Analysis of variance was used to assess whether differences in the number of local lesions produced among the virions (or virion RNA) were statistically different.

DISCUSSION

The studies described here show that a 38-aa sequence encompassing the CNV CP arm region and the adjacent SVRI sequence specifically targets GFP to the chloroplast stroma. Import also occurs in CNV-infected plants, suggesting that CP targeting to chloroplasts represents an important aspect of the CNV infection cycle. We also show that the SVRI sequence is required for efficient targeting but does not appear to affect import across the chloroplast membranes. We also show that a CNV mutant in which the arm is incapable of extrusion to the outside of the virion is less efficient in establishing infection in a local lesion host, consistent with the notion that interaction of the arm region with chloroplasts may play a role in the establishment of infection in host cells.

Similarities between the CNV arm and cellular chloroplast TP sequences. The majority of chloroplast proteins are translated in the cytoplasm as preproteins with amino-terminal TPs

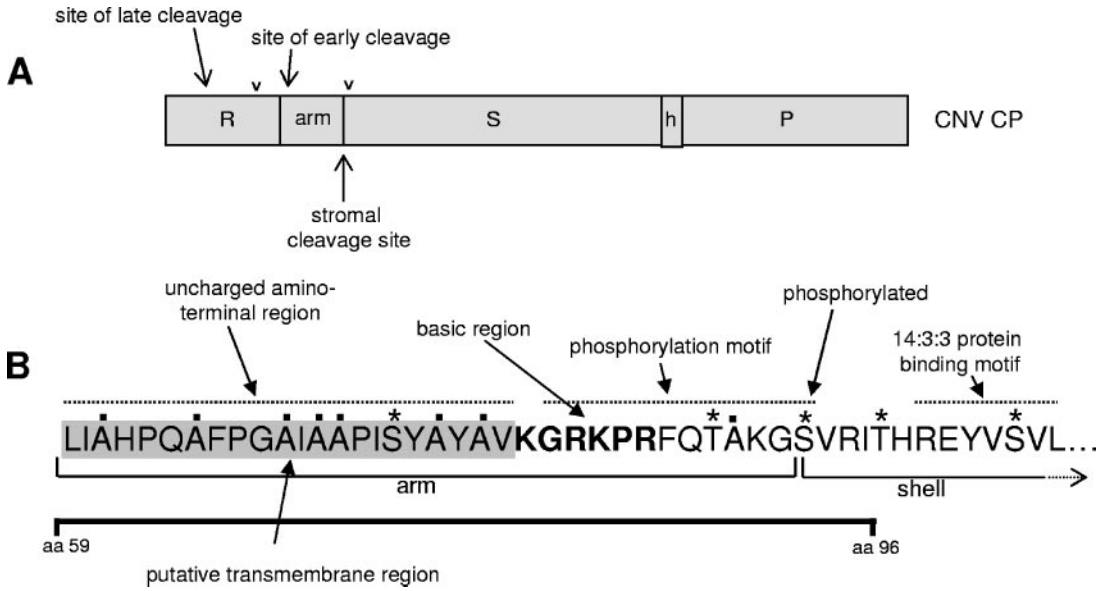

FIG. 10. Features of the CNV CP arm. (A) Approximate positions of protease cleavage sites in the CNV CP R and arm regions along with the proposed cellular sites of cleavage (outside the chloroplast or in the stroma). The carets indicate a region of trypsin-sensitive cleavage sites in swollen CNV particles (i.e., CP aa 40 to 95). (B) Features of the CNV arm and adjacent S domain sequence showing similarity to chloroplast TPs. The complete sequence of the arm and the first 12 aa of the S domain are shown, with the 38-aa region of the sequence that has been identified to function as a chloroplast TP underlined in bold. Regions with similarity to conserved regions of chloroplast TPs are overlined, and features that are similar to chloroplast TPs are indicated. Alanine residues are indicated by dots, and serine residues are indicated by asterisks. Amino acids comprising an internal positively charged region are in bold. The shaded region corresponds to a predicted transmembrane domain, as identified by HMMTOP (G. E. Tusnády [http://www.enzim.hu/hmmtop]).

that direct transport to the chloroplast via specific interaction with various components of the import machinery (2, 37). Little obvious sequence similarity exists among chloroplast TPs; however, common features that relate to their function in transport have been described (43). Most chloroplast TPs are between 25 and 150 aa in length, and most have an amino-terminal region that is uncharged and an internal region that is basic (23, 43). Chloroplast TPs also tend to be rich in serine and threonine, as well as alanine, residues. Some have been found to possess 14-3-3 and HSP70 binding domains (2, 23, 43) that appear to function in part of the targeting process. Finally, phosphorylation motifs as well as specific phosphorylated residues in some TPs have been noted; these appear to regulate the efficiency of preprotein targeting (10, 40). Figure 10 shows the sequence of the region surrounding the CNV arm(+SVRI) sequence, indicating features of the sequence that are similar to those of typical chloroplast TPs. The arm(+SVRI) sequence is 38 aa in length and contains an amino-terminal 22-aa region that is free of charged residues. This region is followed by a 6-aa region that contains 4 positively charged residues. The CNV arm(+SVRI) sequence has a high proportion of alanine residues (8 out of a total of 38 aa). In addition, the region surrounding the CNV arm(+SVRI) sequence contains two conserved motifs previously identified in chloroplast TPs: the sequence *G*RKP*R*GQ*T*AKGS, which conforms to a previously described phosphorylation motif [(P/G)$X^{n(0-3)}$(R/K)$X^{n(0-3)}$(S/T)$X^{n(0-3)}$(pS/pT)] (10, 40), and the sequence *R*EYV*S*VL, which resembles a 14-3-3 binding motif (RX^{n}pSXP) (3, 23) and is present in the S domain sequence just downstream of the delineated TP region (Fig. 10).

The data in Fig. 6 show that the SVRI sequence of the CNV chloroplast TP-like region is required for efficient targeting to chloroplasts. The serine residue of this sequence is part of a predicted phosphorylation motif involved in chloroplast import (23, 40); indeed, we have found that the SVRI serine residue is phosphorylated in capsid protein extracted from CNV virions (D. Rochon, unpublished results). These finding are therefore consistent with a role of the CNV chloroplast TP-like region in the CNV infection process.

Chloroplast TPs have been postulated to interact with the chloroplast outer membrane as part of the initial stages of the import process (6, 30). Consistent with the role of the CNV chloroplast TP-like region in chloroplast targeting is the presence of a predicted transmembrane binding region (Fig. 10) in the first 22 aa of the delineated chloroplast TP-like region that could potentially contribute to the role of the chloroplast TP-like region in chloroplast targeting.

The majority of chloroplast TPs (approximately 82%) contain binding motifs for HSP70, and several have been shown to act as substrates for the binding of HSP70 molecular chaperones (2, 11, 29, 43). This finding suggests that the CNV chloroplast TP-like region may be recognized by a cellular HSP70 protein during infection.

It is known that plant chloroplast TPs must lie in the amino-terminal region of the preprotein in order to function (30, 37, 43). As shown in Fig. 1, we found that when the CNV chloroplast TP-like region sequence was fused to the carboxyl-terminal region of GFP, chloroplast targeting failed to occur. Moreover, GFP constructs in which the R domain lies upstream of the chloroplast TP-like region sequence undergo cleavage in the arm region just outside of the R-arm junction (see below), and it is only this cleavage product that is found to enter

chloroplasts. Thus, circumstantial evidence exists that the CNV CP has evolved a mechanism to position the CNV chloroplast TP-like region sequence at the amino terminus of the CP, presumably to regulate its function as a TP.

The striking number of features common to known chloroplast TPs suggests that the arm(+SVRI) sequence in the CNV CP has evolved to mimic cellular chloroplast TPs and, moreover, that the sequence interacts with several of the various components of the chloroplast import machinery during CNV infection.

Three specific cleavage events occur upon expression of CNV CP in plants. As summarized in Fig. 10A, three specific cleavage events have been found to occur in the CNV CP: one within the R domain sequence; another in the arm, near the R-arm junction; and another near the arm-S junction. The two former cleavages occur outside of the chloroplast, with the cleavage near the R-arm junction occurring earlier in the time course of expression and the cleavage within the R domain occurring later. The third cleavage event occurs within the chloroplast stroma. It is known that cleavage of TPs occurs within the stroma following transport across the chloroplast outer and inner membranes (30); thus, our observation that cleavage occurs in the region just downstream from the CNV chloroplast TP-like region is consistent with its function as a stromal chloroplast TP.

Model for targeting of the CNV CP subunit during infection. Fig. 11A proposes a model for import of the CNV CP into chloroplasts, based on models for import of chloroplast preproteins (2, 35) and the findings reported here. In this model, full-length CNV CP subunit is proteolytically cleaved in the arm domain just downstream of the R-arm junction. Cleavage occurs either in the cytoplasm or in association with a particular organelle outside the chloroplast. The remaining CP sequences (arm/S/P) interact with specific components of the targeting machinery (such as 14-3-3 and HSP70, etc.) to facilitate transport to the chloroplast. Import into the stroma then occurs, presumably via the chloroplast Tic and Toc translocon utilized by other chloroplast preproteins (35). Proteolytic removal of the chloroplast TP-like region near the arm-S junction then occurs via a stromal protease, as has been shown to occur with chloroplast TPs (2, 35).

Potential function of the CNV chloroplast TP-like region during virus infection. Our observations that CNV CP sequences enter chloroplasts during infection and that the CNV arm region can function as a chloroplast TP raises the question as to the potential biological significance of chloroplast targeting during CNV infection. The significance of the chloroplast TP-like region may be via its presence in the CP subunit and/or its presence in virus particles. With regard to the role of the chloroplast TP-like region in CNV CP subunit, it is possible that chloroplasts represent a site for removing excess CP that accumulates during virus infection, as has been suggested for the nuclear inclusion bodies formed during potyvirus infection (28). However, our finding that relatively little CNV CP (1 to 5% of total CP) is found within chloroplasts of CNV-infected leaves makes this seem unlikely. The possibility that the chloroplast TP-like region may function as part of the CNV particle is supported by our observation that particles of the CNV mutant, Pro73Gly, which are defective in externalization of the arm are inefficient in establishing infection even though the corresponding arm-GFP fusion protein is capable of targeting to chloroplasts. The following discusses aspects of the icosahedral particle uncoating process that may be related to the role of the CNV chloroplast TP-like region.

CNV particles, like those of many other small spherical viruses, are known to undergo swelling in vitro in which particles expand and portions of the R and arm regions are extruded to the particle surface (12, 17). A similar expansion occurs during entry and uncoating of poliovirus particles on host cell membranes, prompting the suggestion that particle expansion and R/arm externalization in plant viruses may represent part of the virus uncoating mechanism (14). Indeed, it has been found that swollen particles of several icosahedral plant viruses can be efficiently translated in vitro (4), a finding consistent with the notion that the swollen state may represent an intermediate in the uncoating process. In addition, as described above, during the attachment stage of fungus transmission, CNV particles assume a "swollen-like" conformation which is required for fungus transmission (17, 32). We have recently found that an approximately 54-aa region of the CNV CP, encompassing the last 18 aa of the R domain, the complete arm, and the first 2 aa of the S domain, becomes externalized upon particle swelling in vitro (17). Thus, if CNV particles swell during the infection process, the CNV chloroplast TP-like region would be exposed on the particle surface and thus presumably be accessible to cellular factors that interact with chloroplast TPs.

It is believed that spherical viruses undergo "breathing" in host cells, in which native particles transiently assume a swollen state (5). In the case of CNV, such a transient state would provide an opportunity for interaction of the chloroplast TP-like region with host proteins (such as 14-3-3 and HSP70) and for the various cleavage events described in Fig. 10. The known involvement of HSP70 in macromolecular disassembly (13), along with its role in the targeting process, raises the intriguing possibility that binding of HSP70 to the CNV particle may play a role in CNV disassembly in plant cells.

Hypothetical model for CNV uncoating on chloroplasts. We propose a hypothetical model that outlines possible major steps in CNV particle uncoating during infection (Fig. 11B). This model incorporates observations reported here with respect to similarities between the CNV chloroplast TP-like region and cellular TPs and the three proteolytic cleavages that occur in conjunction with transport, as well as the structural and functional similarities between the CNV and poliovirus capsid described above (14, 17, 32). This model is similar to that shown in Fig. 11A except that it describes events associated with CNV particles rather than CP subunit. As shown in Fig. 11B, we suggest that the transient exposure of the chloroplast TP-like region of the CP that occurs during "breathing" enables proteolytic cleavage in the arm near the R-arm junction, thus placing the CNV chloroplast TP-like region at the amino terminus of the CP and thereby facilitating its function as chloroplast TP. The CNV chloroplast TP-like region then interacts with cytoplasmic factors involved in chloroplast preprotein targeting (such as 14-3-3 and HSP70), and bound particles are targeted to the chloroplast import translocon (Tic and Toc) (23, 35). Import of the arm/S/P region into chloroplasts then drives virus particle disassembly and release of virion RNA on the cytoplasmic side of the chloroplast. We speculate that

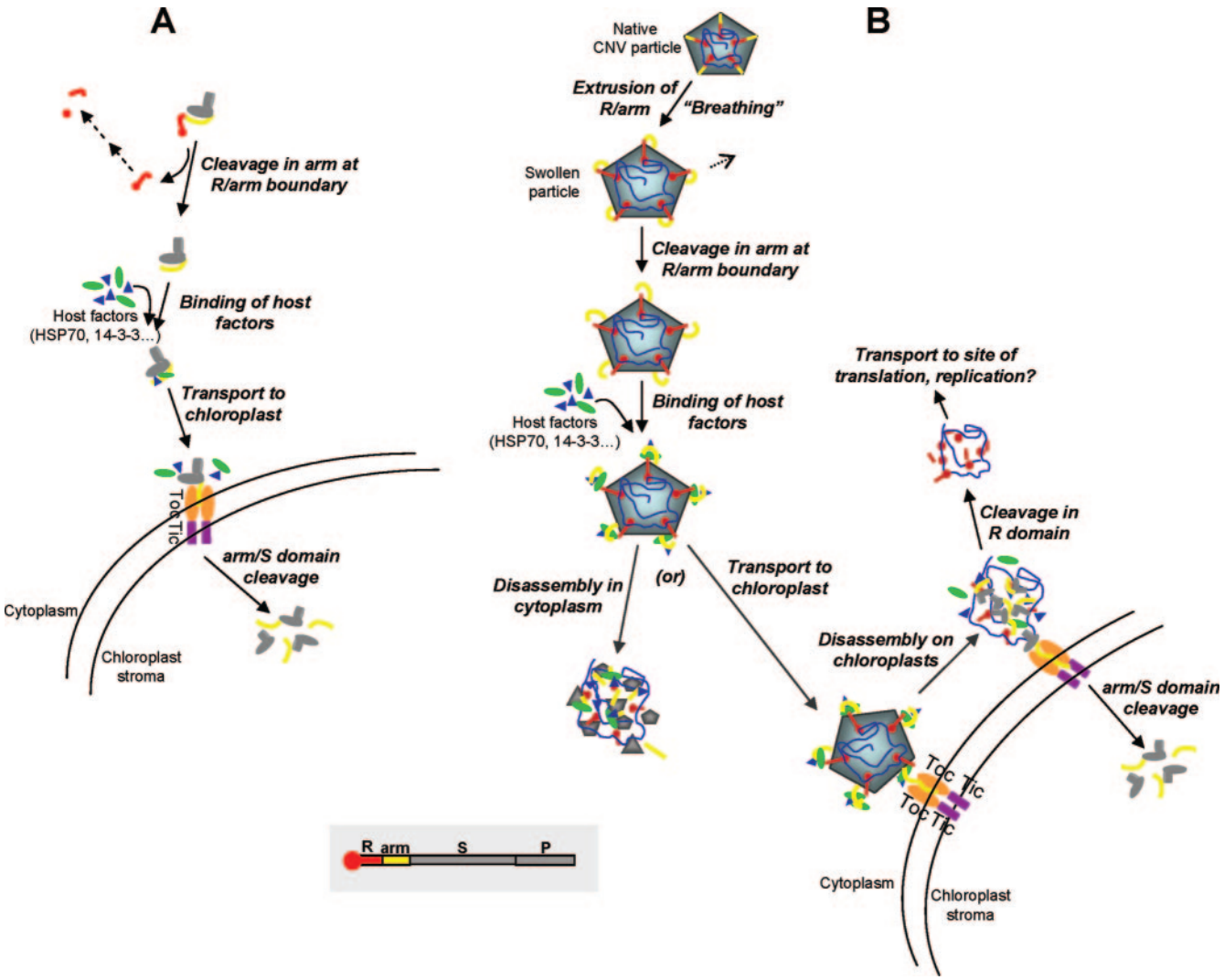

FIG. 11. Hypothetical models for import of CNV CP and CNV particle uncoating on chloroplasts. (A) Import of the CNV CP subunit. A diagram of the folded CNV coat protein subunit is shown, with the R, arm, S, and P domains differentially colored (see key at bottom). The R domain is shown to contain two regions (designated with a line and closed circle) that correspond to the two fragments that are released following proteolytic cleavage (Fig. 10A). Cleavage occurs in the arm at the R-arm boundary, followed by binding of the arm region (the CNV chloroplast TP-like region) by host factors involved in cellular chloroplast preprotein targeting. Transport to and uptake by the chloroplast Tic/Toc translocon occurs, and cleavage by a stromal protease ensues. (B) Diagrammatic representation of the CNV particle, indicating the internal location of the R and arm domains and the encased virion RNA (blue line). Extrusion of the arm and part of the R domain occurs (due to "breathing" of particles). This is followed by proteolytic cleavage in the arm near the R-arm junction (Fig. 10A) and binding by host factors involved in cellular chloroplast protein import, as described above for the CP subunit. Two potential routes for disassembly of the host protein-bound particle are shown. Disassembly in the cytoplasm would be driven by binding of host factors such as HSP70 and 14-3-3. Alternatively, the particle complex could be transported to the chloroplast, whereupon uptake of the arm/S/P region of the particle facilitates the disassembly process on the cytoplasmic side. Virion RNA is released as an R domain-RNA complex wherein the R domain is proteolytically cleaved (Fig. 10A) and transported to the site of RNA translation and/or replication. The imported arm/S/P region of the particle subunit is cleaved as described above.

virion RNA may remain bound to the previously cleaved region of the R domain upon uncoating and that the R domain-virion RNA complex could then be targeted to the site of translation (and/or replication).

It is also possible that binding of the exposed arm region by cellular TP binding proteins in the cytoplasm (such as 14-3-3 proteins and HSP70) could itself facilitate particle disassembly, thus obviating the need for particles to target chloroplasts. This possibility should be considered, especially in light of the fact that HSP70 has a known function in the disassembly of oligomeric proteins (15, 29).

The overall features of this proposed model may be applicable to a number of plant viruses with spherical capsids, although the site of uncoating and details of the uncoating process may differ. Additionally, there are still many components of the proposed uncoating events that require further experimental analyses. The model shown in Fig. 11 should facilitate the design of such experiments so that the model can be validated and refined.

ACKNOWLEDGMENTS

We thank Michael Weis for expert guidance with regard to confocal microscopy.

This work was supported in part by NSERC operating grant 43840.

REFERENCES

1. **Ahlquist, P.** 2002. RNA-dependent RNA polymerases, viruses, and RNA silencing. Science **296:**1270–1273.
2. **Bedard, J., and P. Jarvis.** 2005. Recognition and envelope translocation of chloroplast preproteins. J. Exp. Bot. **56:**2287–2320.
3. **Bridges, D., and G. B. Moorhead.** 2005. 14-3-3 proteins: a number of functions for a numbered protein. Sci. STKE **2005:**re10.
4. **Brisco, M. J., R. Hull, and T. M. A. Wilson.** 1985. Southern bean mosaic virus-specific proteins are synthesized in an in vitro system supplemented with intact, treated virions. Virology **143:**392–398.
5. **Broo, K., J. Wei, D. Marshall, F. Brown, T. J. Smith, J. E. Johnson, A. Schneemann, and G. Siuzdak.** 2001. Viral capsid mobility: a dynamic conduit for inactivation. Proc. Natl. Acad. Sci. USA **98:**2274–2277.
6. **Bruce, B. D.** 2000. Chloroplast transit peptides: structure, function and evolution. Trends Cell Biol. **10:**440–447.
7. **Bruce, B. D., S. Perry, J. Froehlich, and K. Keegstra.** 1994. Plant molecular biology manual, 2nd ed., vol. J1, p. 1–15. Kluwer Academic Publishers, Boston, Mass.
8. **Burgyan, J., L. Rubino, and M. Russo.** 1996. The 5′-terminal region of a tombusvirus genome determines the origin of multivesicular bodies. J. Gen. Virol. **77:**1967–1974.
9. **Desvoyes, B., S. Faure-Rabasse, M. H. Chen, J. W. Park, and H. B. Scholthof.** 2002. A novel plant homeodomain protein interacts in a functionally relevant manner with a virus movement protein. Plant Physiol. **129:**1521–1532.
10. **Fulgosi, H., and J. Soll.** 2002. The chloroplast protein import receptors Toc34 and Toc159 are phosphorylated by distinct protein kinases. J. Biol. Chem. **277:**8934–8940.
11. **Gottesman, M. E., and W. A. Hendrickson.** 2000. Protein folding and unfolding by Escherichia coli chaperones and chaperonins. Curr. Opin. Microbiol. **3:**197–202.
12. **Harrison, S. C.** 1983. Virus structure: high-resolution perspectives. Adv. Virus Res. **28:**175–240.
13. **Hartl, F. U.** 1996. Molecular chaperones in cellular protein folding. Nature **381:**571–580.
14. **Hogle, J. M.** 2002. Poliovirus cell entry: common structural themes in viral cell entry pathways. Annu. Rev. Microbiol. **56:**677–702.
15. **Ivey, R. A., III, C. Subramanian, and B. D. Bruce.** 2000. Identification of a Hsp70 recognition domain within the rubisco small subunit transit peptide. Plant Physiol. **122:**1289–1299.
16. **Jackson, D. T., J. E. Froehlich, and K. Keegstra.** 1998. The hydrophilic domain of Tic110, an inner envelope membrane component of the chloroplastic protein translocation apparatus, faces the stromal compartment. J. Biol. Chem. **273:**16583–16588.
17. **Kakani, K., R. Reade, and D. Rochon.** 2004. Evidence that vector transmission of a plant virus requires conformational change in virus particles. J. Mol. Biol. **338:**507–517.
18. **Kakani, K., J. Y. Sgro, and D. Rochon.** 2001. Identification of specific cucumber necrosis virus coat protein amino acids affecting fungus transmission and zoospore attachment. J. Virol. **75:**5576–5583.
19. **Lakatos, L., G. Szittya, D. Silhavy, and J. Burgyan.** 2004. Molecular mechanism of RNA silencing suppression mediated by p19 protein of tombusviruses. EMBO J. **23:**876–884.
20. **Lazarowitz, S. G., and R. N. Beachy.** 1999. Viral movement proteins as probes for intracellular and intercellular trafficking in plants. Plant Cell **11:**535–548.
21. **Liu, Y., M. Schiff, and S. P. Dinesh-Kumar.** 2002. Virus-induced gene silencing in tomato. Plant J. **31:**777–786.
22. **Lubeck, J., L. Heins, and J. Soll.** 1997. A nuclear-coded chloroplastic inner envelope membrane protein uses a soluble sorting intermediate upon import into the organelle. J. Cell Biol. **137:**1279–1286.
23. **May, T., and J. Soll.** 2000. 14-3-3 proteins form a guidance complex with chloroplast precursor proteins in plants. Plant Cell **12:**53–64.
24. **McLean, M. A., R. N. Campbell, R. I. Hamilton, and D. M. Rochon.** 1994. Involvement of the cucumber necrosis virus coat protein in the specificity of fungus transmission by Olpidium bornovanus. Virology **204:**840–842.
25. **McLean, M. A., R. I. Hamilton, and D. M. Rochon.** 1993. Symptomatology and movement of a cucumber necrosis virus mutant lacking the coat protein protruding domain. Virology **193:**932–939.
26. **Panavas, T., C. M. Hawkins, Z. Panaviene, and P. D. Nagy.** 2005. The role of the p33:p33/p92 interaction domain in RNA replication and intracellular localization of p33 and p92 proteins of Cucumber necrosis tombusvirus. Virology **338:**81–95.
27. **Prod'homme, D., A. Jakubiec, V. Tournier, G. Drugeon, and I. Jupin.** 2003. Targeting of the *Turnip yellow mosaic virus* 66K replication protein to the chloroplast envelope is mediated by the 140K protein. J. Virol. **77:**9124–9135.
28. **Restrepo, M. A., D. D. Freed, and J. C. Carrington.** 1990. Nuclear transport of plant potyviral proteins. Plant Cell **2:**987–998.
29. **Rial, D. V., A. K. Arakaki, and E. A. Ceccarelli.** 2000. Interaction of the targeting sequence of chloroplast precursors with Hsp70 molecular chaperones. Eur. J. Biochem. **267:**6239–6248.
30. **Rial, D. V., J. Ottado, and E. A. Ceccarelli.** 2003. Precursors with altered affinity for Hsp70 in their transit peptides are efficiently imported into chloroplasts. J. Biol. Chem. **278:**46473–46481.
31. **Robinson, I. K., and S. C. Harrison.** 1982. Structure of the expanded state of tomato bushy stunt virus. Nature **297:**563–568.
32. **Rochon, D., K. Kakani, M. Robbins, and R. Reade.** 2004. Molecular aspects of plant virus transmission by olpidium and plasmodiophorid vectors. Annu. Rev. Phytopathol. **42:**211–241.
33. **Rochon, D. M., and J. C. Johnston.** 1991. Infectious transcripts from cloned cucumber necrosis virus cDNA: evidence for a bifunctional subgenomic mRNA. Virology **181:**656–665.
34. **Schaad, M. C., P. E. Jensen, and J. C. Carrington.** 1997. Formation of plant RNA virus replication complexes on membranes: role of an endoplasmic reticulum-targeted viral protein. EMBO J. **16:**4049–4059.
35. **Schleiff, E., and J. Soll.** 2000. Travelling of proteins through membranes: translocation into chloroplasts. Planta **211:**449–456.
36. **Sit, T. L., J. C. Johnston, M. G. ter Borg, E. Frison, M. A. McLean, and D. Rochon.** 1995. Mutational analysis of the cucumber necrosis virus coat protein gene. Virology **206:**38–48.
37. **Soll, J., and E. Schleiff.** 2004. Protein import into chloroplasts. Nat. Rev. Mol. Cell Biol. **5:**198–208.
38. **van Engelen, F. A., J. W. Molthoff, A. J. Conner, J. P. Nap, A. Pereira, and W. J. Stiekema.** 1995. pBINPLUS: an improved plant transformation vector based on pBIN19. Transgenic Res. **4:**288–290.
39. **Vargason, J. M., G. Szittya, J. Burgyan, and T. M. Tanaka Hall.** 2003. Size selective recognition of siRNA by an RNA silencing suppressor. Cell **115:**799–811.
40. **Waegemann, K., and J. Soll.** 1996. Phosphorylation of the transit sequence of chloroplast precursor proteins. J. Biol. Chem. **271:**6545–6554.
41. **Weber-Lotfi, F., A. Dietrich, M. Russo, and L. Rubino.** 2002. Mitochondrial targeting and membrane anchoring of a viral replicase in plant and yeast cells. J. Virol. **76:**10485–10496.
42. **Ye, K., L. Malinina, and D. J. Patel.** 2003. Recognition of small interfering RNA by a viral suppressor of RNA silencing. Nature **426:**874–878.
43. **Zhang, X. P., and E. Glaser.** 2002. Interaction of plant mitochondrial and chloroplast signal peptides with the Hsp70 molecular chaperone. Trends Plant Sci. **7:**14–21.